Biophysical Chemistry, 45 (1992) 17–25
Elsevier Science Publishers B.V., Amsterdam

BIOCHE 01693

Structure and dynamics of motilin. Time-resolved fluorescence of peptide hormone with single tyrosine residue

B.-M. Backlund and A. Gräslund

Department of Medical Biochemistry and Biophysics, University of Umeå, S-901 87 Umeå (Sweden)

(Received 6 March 1992; accepted 11 June 1992)

Abstract

Time-resolved fluorescence and CD spectroscopy were used to characterize the structure and dynamics of the peptide hormone motilin with a single tyrosine residue among its 22 amino acids. CD spectroscopy showed that secondary structure is independent of concentration in the range $1 \cdot 10^{-5}$–$2.6 \cdot 10^{-4}$ M, and of the presence of DOPC lipid vesicles, but is strongly induced by addition of hexafluoroisopropanol. The fluorescence studies with tyrosine as the intrinsic fluorophore, performed at the MAX synchrotron laboratory at Lund, showed that three fluorescence lifetimes (0.4 ns, 1.7 ns and 3.6 ns at 20°C) and two rotational correlation times (0.4 ns and 5 ns at 20°C) were needed to account for the data. The different decay times are interpreted as representing ground-state rotamers interconverting slowly on the ns time scale. The rotational correlation times are ascribed to local angular motion of the tyrosyl ring, and global motion of the whole peptide, respectively.

Keywords: Time-resolved fluorescence; Tyrosine; Motilin; Circular dichroism; Liposomes

1. Introduction

Motilin is a small peptide hormone consisting of 22 amino acid residues (for a survey on motilin, see ref. [1]). It was first isolated by Brown et al. [2] from duodenal mucosa. Its primary function in the gut appears to be to regulate the migrating motor complex [3,4]. Receptors of motilin have been found to be membrane bound in the smooth muscle tissue of the gastrointestinal tract [5–7].

Correspondence to: Professor Astrid Gräslund, Department of Medical Biochemistry and Biophysics, University of Umeå, S-901 87 Umeå (Sweden).

Motilin was first isolated from pig, and its sequence is FVPIFTYGELQRMQEKERNKGQ [2,8]. The amino acid sequence of human motilin has been deduced from studies of an intestinal cDNA clone coding for the human motilin precursor protein, and was found to be identical to that of porcine motilin [9]. Canine motilin on the other hand, differs from porcine motilin in five positions, among them Tyr-7, which is replaced by histidine [10].

The three-dimensional structure of motilin in solution has recently been elucidated through two-dimensional ^{1}H-NMR studies [11] followed by structure calculations [12]. The results in an aqueous solvent containing 30% hexafluoroiso-

Fig. 1. Superposition of ten motilin solution structures of the peptide backbone from Distance Geometry calculations [12]. Residues 8–20 have been aligned for best fit of peptide backbone atoms. The N- and C-terminals are indicated. The arrow indicates the Tyr-7 residue.

propanol showed that the C-terminal end of the molecule (residues 9 to 19) forms a relatively stable α-helix, whereas residues 3–6 form a wide turn (Fig. 1).

The region around Tyr-7 is not well defined by the ^{1}H-NMR results which was tentatively ascribed to a highly dynamic "hinge-like" behaviour of this part of the peptide chain [11]. The mixed solvent was chosen since it allowed a fairly stable structure to be formed (verified by CD studies) which enabled the ^{1}H-NMR structure determination.

Studies on synthetic fragments of motilin have indicated that the N-terminal end of the molecule is particularly important for activity [13,14]. A residue 1–5 fragment has the ability to bind to the motilin receptor [15].

The present work aims at a spectroscopic characterization of motilin, combined with the use of Tyr-7 as an intrinsic fluorescence probe to study the dynamics of the molecule through time-resolved fluorescence. Parallel observations in an aqueous solution with and without HFP were made to probe the effect on the spectroscopic parameters of the stabilization of secondary structure effected by HFP. Studies of fluorescence decay and fluorescence polarization anisotropy decay were performed at the MAX-synchrotron laboratory, Lund, Sweden, using the synchrotron light as the pulsed excitation source.

2. Materials and methods

Porcine motilin was kindly provided by professor Viktor Mutt, Karolinska Institutet. The normal solvent was 20 m*M* acetic acid, which had a pH around 3.5. For confirmation of composition and determination of extinction coefficient, a light absorption spectrum was recorded (see below) and aliquots of 30 μl containing about 10 μg of peptide were transferred to amino acid analysis tubes and frozen. These samples were subsequently hydrolysed in 6 *M* constant boiling HCl, at 110°C for 24 h, and lyophilized. The amino acids were quantitated by using a Biotronic LC 5000, with a Shimadzu C-R2AX data module. The mass of the sample was calculated using the mean abundance of the following amino acids: Val, Met, Ile, Leu, Tyr, which varied around an average within $\pm 5\%$.

Hexafluoropropanol-2, $(CF_3)_2CHOH$ (HFP) was obtained from Sigma Ltd. Dioleylphosphatidyl choline (DOPC) vesicles were prepared from 1,2-dioleyl-*sn*-glycero-3-phosphocholine (Avanti Polar Lipids, USA) as previously described [16,17].

Light absorption measurements were carried out in a CARY 4 spectrophotometer normally using cuvettes with 2 mm light path. Spectra were baseline corrected and derivatives were calculated using the CARY software. The temperature was regulated using a thermostatted water bath.

CD measurements were carried out using a JASCO J-700 spectropolarimeter and normally cuvettes with a 2 mm light path. Spectra were baseline corrected and also corrected for dilution during titrations with hexafluoroisopropanol using the spectrometer software. The temperature was controlled using a digital control device cooling or heating the cuvette house.

Static fluorescence spectra were measured using a Shimadzu RF 5000 spectrofluorometer, using a 10 mm cuvette, and temperature regulation by a thermostatted water bath.

Time-resolved fluorescence and fluorescence polarization anisotropy measurements were carried out at the MAX synchrotron laboratory, Lund, Sweden [18]. The synchrotron operating in the single bunch mode had a light pulse with a Gaussian shape and a variance of 60 ps. A monochromator with a band width of 9 nm was used on the excitation side, whereas edge filters (high wavelength pass) from Schott-Jena were used on the emission side for optimum fluorescence signal intensity. Polarized and unpolarized components of the decay were measured by the time-correlated single photon counting technique using a microchannel plate detector. The temperature was regulated by a thermostatted water bath.

Four different data sets were collected [19,20]: synchrotron light, dark current, $I_\perp$ and I_m, where $I_\perp$ is the perpendicular intensity and I_m is the magic angle intensity relative to the polarization of the exciting light pulse. The decay was followed for 40 ns and the synchrotron pulses were repeated every 108 ns. The time spent on each measurement was typically one hour, cycling through collection in the different data sets every 80 sec.

The analysis of the data is based on the concept of discrete fluorescence decay and polarization anisotropy decay components and was described in [20,21]. Some important features are summarized here.

Fluorescence decays $I_m(t)$ were described as a sum of discrete exponential components

$$I_m(t) = \sum_i \alpha_i \exp(-t/\tau_i) \quad (1)$$

τ_i is a fluorescence lifetime and α_i its amplitude.

The decay of fluorescence polarization anisotropy of the system is a function of the rotational correlation times as well as of the fluorescence decay times. The rotational correlation times ρ_i were evaluated under the assumption that each rotational component is associated with all decay components (previously determined) through

$$\frac{I_\perp(t)}{I_m(t)} = 1 - \frac{\left(\sum_i \beta_i \exp(-t/\rho_i)\right)\left(\sum_j \alpha_j \exp(-t/\tau_j)\right)}{\sum_j \alpha_j \exp(-t/\tau_j)} \quad (2)$$

β_i is the zero-time anisotropy for component i and ρ_i is the corresponding rotational correlation time. The χ^2 value indicates goodness of fit between model and experiments, and should be close to 1 (e.g. below 1.5) when no significant systematic deviations appear between model and experiments. As discussed in [21] rather large

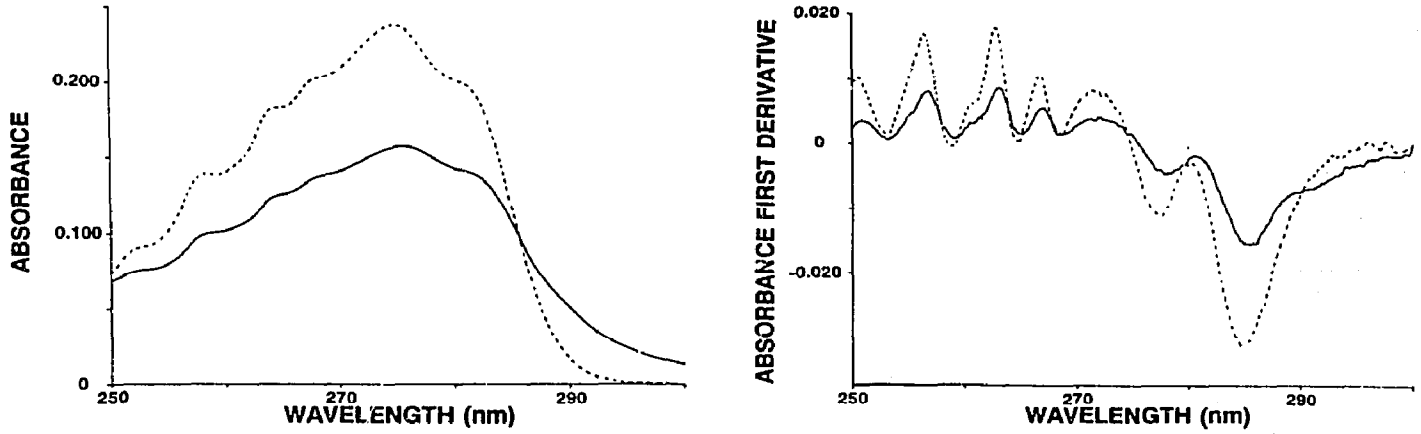

Fig. 2. Light absorption (left) and first derivative (right) spectra of motilin with concentration $3.1 \cdot 10^{-4}$ M (—) and 1:2 (tyr:phe) mixture with concentration $8.3 \cdot 10^{-4}$ M (- - -) in 20 mM acetic acid solution (pH 3).

uncertainties are associated with the estimated parameters, mainly due to the rather low light intensity of the synchrotron beam. Particularly the anisotropy decay parameters (rotational correlation times) should be considered correct within ±50% only.

3. Results and discussion

3.1 Light absorption

Motilin contains three aromatic residues: Phe-1, Phe-5 and Tyr-7. Figure 2 shows light absorption and first derivative spectra of motilin. The shape of the spectra are in qualitative agreement with those of a 1:2 (Tyr:Phe) mixture in aqueous solution also included in Fig. 2. Two vibrational components of tyrosine can be distinguished above 270 nm and four components of phenylalanin below 270 nm. In the derivative spectra we evaluated successive maxima and minima (Table 1). Compared to the maxima and minima in 1:2 Tyr:Phe solution the corresponding light absorption bands in motilin are shifted a few tenths of an Ångström towards longer wavelengths for both tyrosine and phenylalanin. The positions of the bands of the mixed amino acid solution correspond within 0.5 nm to those reported in [22] for pure amino acids in water. The small but significant shifts towards longer wavelengths particularly of the tyrosine light absorption in motilin suggests a somewhat higher polarizability and polarity in its environment relative to that in water.

An absorbance index of motilin at 275 nm, ϵ_{275} was determined by performing light absorption measurements and amino acid analysis on the same samples. We evaluated $\epsilon_{275} = 2300\ M^{-1}\ cm^{-1}$ at 22°C. This value is higher than for tyrosine alone in solution ($\epsilon_{275} = 1450\ M^{-1}\ cm^{-1}$, ref. [22]), possibly in part due to the presence of the two phenylalanine residues. No measurable amounts of contaminating tryptophan was-observed in the amino acid analysis, indicating a fairly pure preparation of native motilin.

3.2 CD spectroscopy

Previous studies have shown that addition of HFP induces α-helical secondary structure in motilin, from about 20% in 0% HFP to 50% in 30% HFP, at 22°C, the latter estimation in good agreement with the NMR structure results in 30% HFP [11]. The estimation was based on the assumption that only α-helix and random coil secondary structures were present.

A question raised by the NMR results concerned the possible presence of motilin dimers at mM concentrations. We therefore studied the temperature dependence of motilin CD spectra, at a high ($2.6 \cdot 10^{-4}\ M$) and a low ($1.0 \cdot 10^{-5}\ M$) concentration and at 0% HFP and 30% HFP. Figure 3 shows CD spectra at the two concentrations at 5°C and 60°C, respectively, without and with 30% HFP. It can be seen that the behaviour at the two concentrations is virtually identical, supporting the tentative conclusion from the NMR study that motilin exists mainly as a

Table 1

Vibrational maxima and minima in the first derivative light absorption spectrum of motilin and a (1:2) (Tyr:Phe) solution in 20 mM acetic acid at 22°C. The four absorption bands of Phe and two bands of Tyr are presented

Sample	Designation	Wavelength (nm)					
		Phe				Tyr	
		1	2	3	4	1	2
Motilin	Maximum	251.0	256.8	263.1	267.0	271.9	280.5
	Minimum	253.2	259.3	265.2	268.9	278.3	285.4
(1:2) (Tyr:Phe)	Maximum	250.6	256.5	262.8	266.7	271.7	280.1
	Minimum	253.0	258.9	264.8	268.5	277.3	284.9

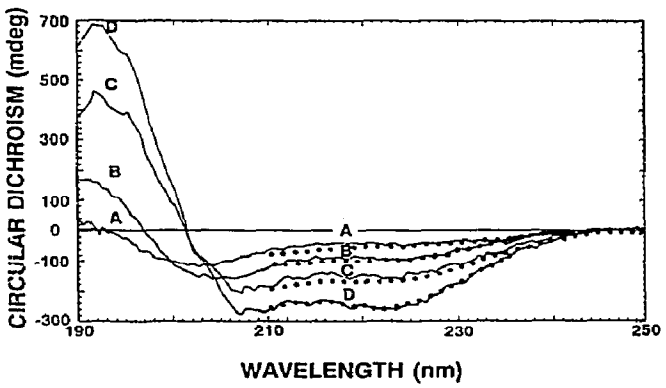

Fig. 3. Circular dichroism spectra for motilin at two concentrations $1.0 \cdot 10^{-5}$ M (—) and $2.6 \cdot 10^{-4}$ M (···) in 20 mM acetic acid, pH 3 at 5°C and 60°C, with and without 30% HFP. (*A*) 0% HFP, 60°C; (*B*) 0% HFP, 5°C; (*C*) 30% HFP, 60°C; (*D*) 30% HFP, 5°C. The spectra obtained at lower concentrations were corrected with respect to dilution.

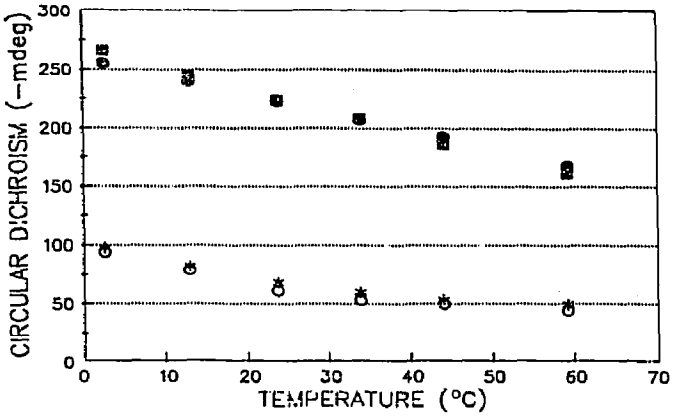

Fig. 4. The temperature dependence of the ellipticity of motilin at two concentrations, with and without 30% HFP (*) $2.6 \cdot 10^{-4}$ M, 0% HFP; (○) $1.0 \cdot 10^{-5}$ M, 0% HFP, signal corrected with respect to dilution; (●) $2.6 \cdot 10^{-4}$ M, 30% HFP, (■) $1.0 \cdot 10^{-5}$ M, 30% HFP, corrected with respect to dilution.

monomer in solution [11]. Fig. 4 shows the temperature dependence of the ellipticity at 222 nm (where the presence of α-helix is most easily seen in CD spectra). In water the θ_{222} reaches a constant low value between about 40°C and 60°C. The corresponding CD spectra at 60°C independent of concentration may be ascribed to a melted fairly "random" structure of the peptide chain. In HFP, there appears to be considerable remaining secondary structure also at 6°C.

In a separate experiment, vesicles formed by the neutral phospholipid DOPC were added to motilin to investigate a possible lipid membrane association accompanied by induction of secondary structure (Fig. 5). However, no significant change was observed in the CD spectra after addition of DOPC. This is in marked contrast to peptides like apolipoprotein CII, which are known to be membrane-associated and showed a signifi-

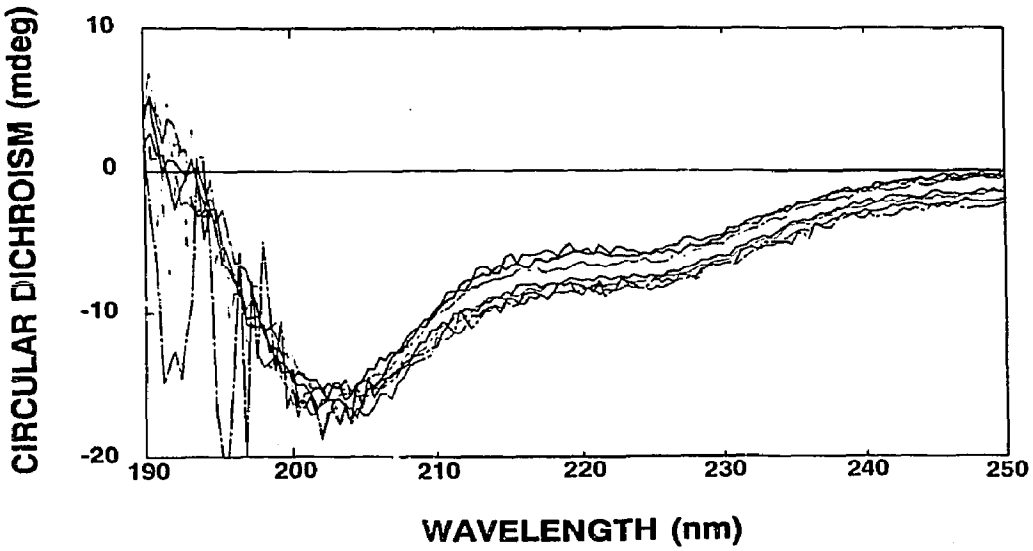

Fig. 5. Circular dichroism spectra of motilin, 400 μg/ml, titrated with DOPC vesicles. The concentration of the vesicles was gradually varied from 0 to 2 mg/ml (top to bottom).

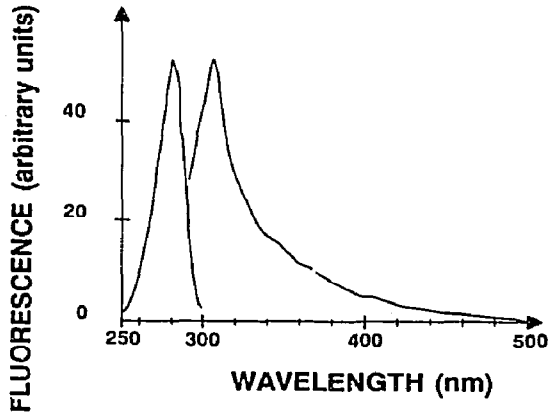

Fig. 6. Excitation (left) and emission (right) spectra of motilin (15 μg/ml) at 22°C. $\lambda_{em} = 305$ nm for the excitation spectrum and $\lambda_{ex} = 280$ nm for the emission spectrum.

cant change of CD spectra reflecting an increased amount of α-helix when DOPC lipid vesicles were added [17].

3.3 Fluorescence spectroscopy

Fluorescence excitation and emission spectra of motilin are shown in Fig. 6. As expected the fluorescence is dominated by tyrosin fluorescence with $\lambda_{max} = 280$ nm for the excitation spectrum and $\lambda_{max} = 305$ nm for the emission spectrum.

Fluorescence decay curves (Fig. 7) and fluorescence polarization anisotropy decay curves (Fig. 8) were studied using synchrotron light as excitation at the MAX synchrotron laboratory at Lund, Sweden. The fluorescence decay of tyrosine alone at 20°C is adequately described as a single-exponential process with a time constant of about 3.2 ns (20 mM acetic acid) or 3.6 ns (with 30% HFP) (data not shown) in reasonable agreement with the lifetime of 3.8 ns reported in [23]. For the motilin sample at least three lifetime components are needed to describe the fluorescence decay process (Table 2). Fitting a model using only two components gives $\chi^2 > 3$ indicating a non-random deviation between model and experimental results.

Addition of HFP to the solvent did not significantly change the pattern of fluorescence decay times or amplitudes. The longest lifetime is similar to that observed for tyrosine alone in solution.

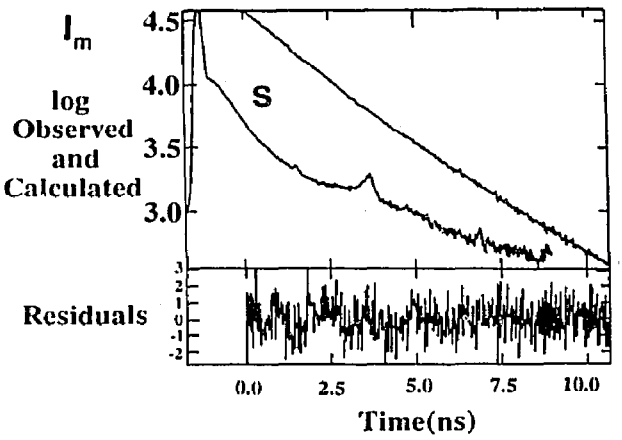

Fig. 7. Fluorescence decay curve (magic angle intensity I_m) of motilin at 20°C. The motilin concentration was $2 \cdot 10^{-4}$ M in 20 mM acetic acid (pH 3). The excitation wavelength was 280 nm. In the upper part of the figure the decay curve is shown together with the synchrotron pulse (denoted S). The vertical scale is light intensity in logarithmic units. The calculated fitted decay curve is almost completely hidden below the experimental one. The residuals (in non-logarithmic vertical scale) between observed and fitted curves are shown at the bottom of the figure.

When the temperature was varied, certain variations were observed in the decay times (Table 2): particularly the two longest ones became smaller towards higher temperatures. Their relative am-

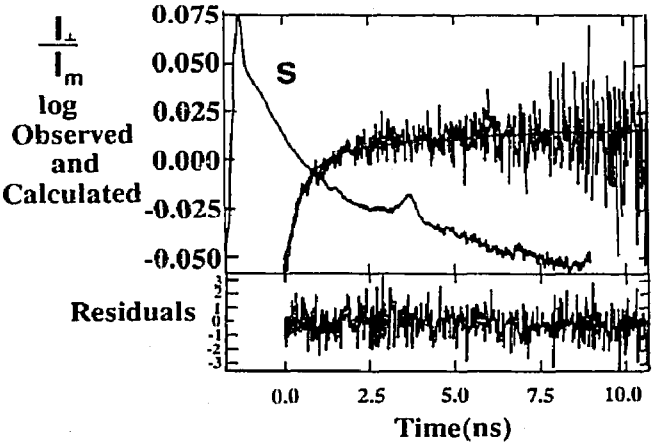

Fig. 8. Fluorescence polarization anisotropy decay curves of motilin measured as ($I_\perp / I_m$) at 20°C. The experimental conditions were as in Fig. 7. In the upper part the anisotropy decay curve is shown together with the synchrotron pulse (denoted S). The calculated fitted curve is partly hidden below the experimental one. The residuals between observed and fitted curves are shown at the bottom of the figure.

plitudes changed so that the smallest lifetime had a relatively larger amplitude at the higher temperatures.

Different mechanisms have been suggested and discussed for quenching of tyrosine fluorescence in proteins with a single tyrosine residue (and no tryptophan) [24]. First, there is the overall observation that more than one lifetime appears. Second, there is the question of the actual lifetime of each component, and third the amplitude associated with each component lifetime. Similar lifetime distributions as described here have been observed previously for single-tyrosine proteins [24–26], and even more often for single-tryptophan proteins [24].

The first observation has been suggested to be due to the existence of ground-state rotamers interconverting slowly on the nanosecond time scale [27], further supported by NMR evidence [23,28]. Answers to the second and third questions are linked to the first one by suggestions of different chemical environments that lead to variable quenching and stabilization of each rotameric state. Among quenching mechanisms, transient H bond formation as well as proton or electron transfer have been discussed [23–28].

Our data encompass a wide variety of experimental conditions, which favour a rather highly structured peptide molecule at low temperatures in 30% HFP, or more or less random coil structures in aqueous solution at higher temperatures. Still the lifetime pattern for all decay curves of motilin (but not the amplitudes) resembles that of the well-structured protein calbindin [26]. The only reasonable interpretation of these observations is that the overall appearance of a lifetime distribution is an inherent property of tyrosine in any polypeptide environment, and is indeed caused by the existence of slowly interconverting rotameric ground-states. How the corresponding amplitudes appear and differ between proteins and varying conditions may depend on local interactions in their turn depending on structure, which should give different weights to and affect the lifetimes of each different rotameric state. We should also note that in our experiments dynamic quenching (through increased mobility) should become more important towards the higher temperatures, which might explain the overall shortening of the lifetimes as the temperature is increased.

The fluorescence polarization anisotropy decay was measured as $\log(I_\perp/I_m)$, where $I_\perp$ and I_m are the intensities measured with polarization perpendicular to and at the magic angle, relative to the polarization of the exciting light pulse. At least two rotational correlation times were needed to describe the decay processes, 0.4 ns and 5.0 ns in acetic acid and 0.5 ns and 6.0 ns with HFP added (Table 3). With 30% HFP the relative amplitude for the shorter correlation time is significantly decreased.

A straightforward interpretation of the rotational correlation times is that the short and long correlation times correspond to local motion of the tyrosyl ring and an overall motion of the whole motilin molecule, respectively. In the previous NMR study the rotational correlation time

Table 2

Fluorescence decay components (amplitudes α_i and decay times τ_i) for motilin in 20 mM acetic acid with or without 30% hexafluoropropanol-2 (HFP) at different temperatures. Excitation wavelength 280 nm. The amplitudes have been normalized so that their sum is 1

HFP (%)	Temperature (°C)	Amplitude			Decay time (ns)			χ^2
		α_1	α_2	α_3	τ_1	τ_2	τ_3	
0	5	0.27	0.50	0.23	0.36	1.81	4.27	1.28
	20	0.30	0.56	0.14	0.40	1.69	3.55	2.21
	40	0.37	0.56	0.07	0.34	1.41	2.51	1.07
30	5	0.32	0.53	0.15	0.48	1.89	4.27	0.96
	20	0.38	0.49	0.13	0.37	1.51	3.69	1.94
	40	0.51	0.42	0.07	0.34	1.50	3.04	1.06

Table 3

Fluorescence polarization anisotropy decay components (amplitudes β_i and rotational correlations times ρ_i) for motilin in 20 mM acetic acid with or without 30% hexafluoropropanol-2 (HFP) at 20°C. Excitation wavelength 280 nm

HFP (%)	Amplitude		Rot. corr. time (ns)		χ^2
	β_1	β_2	ρ_1	ρ_2	
0	0.13	–	–	1.11	1.73
	0.12	0.04	4.98	0.35	1.10
30	0.12	–	–	3.40	1.34
	0.06	0.09	5.95	0.49	1.07

for the motilin α-helical backbone was evaluated to be 2–3 ns, comparable with an estimation based on a model assuming an isotropic rotor [11]. The present result yielding 5–6 ns for the whole motilin molecule is probably correct within 50% and is in reasonable agreement with the NMR results.

The relative size of the amplitude for the rapid motion reflects the restrictions on the local angular motion of the tyrosyl ring through

$$\cos^2\gamma = (2\beta_2 + 1)/3,$$

where $\cos^2\gamma$ is an average value, and γ is the angular displacement characteristic of the rapid motion [29]. A smaller relative amplitude for the rapid motion means more restricted local motion of the tyrosyl ring. Thus our results indicate that the local motion of Tyr-7 is more restricted in 30% HFP solvent than it is in pure 20 mM acetic acid. This is not unreasonable, since CD and NMR studies have already shown that a more well-defined structure is stabilized in the peptide by adding HFP to the solvent [11,12].

In conclusion, this study uses optical spectroscopy and particularly the fluorescence of Tyr-7 to investigate the structural and dynamic properties of motilin in solution. The conditions are widely varied from those employed in the previous NMR studies of the equilibrium conformation in solution. The peptide is most likely a monomer in solution [11,12]. The results indicate that motilin exists in an equilibrium between slowly interconverting (on the ns time scale) rotameric ground states stabilized through local interactions in the structure. Addition of HFP has little influence on the fluorescence characteristics of Tyr-7, although significant effects are observed on the average secondary structure of the peptide chain, as evidenced by CD. These changes may primarily involve parts of the peptide chain that do not include Tyr-7. Local motion of the tyrosyl ring is observed with a rotational correlation time of 400–500 ps at room temperature. The local motion became more restricted in space when HFP was added to the solvent.

Acknowledgements

This study was supported by the Swedish Natural Science Research Council and Magn. Bergwalls Stiftelse. We are grateful to Dr. R. Rigler and Mr. J. Roslund for help regarding the use of the beamline for time-resolved spectroscopy at the MAX synchrotron laboratory, to Mr. J. Zdunek for help in preparing the figure of motilin structure, and to Dr. L.B.Å. Johansson for providing the DOPC vesicles. We thank Dr. P.-I. Ohlsson for help with the amino acid analysis.

References

1 Z. Itoh in: Motilin, ed. Z. Itoh (Academic Press, San Diego, CA, 1990).
2 J.C. Brown, M.A. Cook and J.R. Dryburgh, Can. J. Biochem. 51 (1973) 533.
3 Z. Itoh, R. Aizawa, S. Takeuchi and E.F. Couch, Proc. Int. Symp. Gastrointest. Motility 5th, p. 48.
4 G. Vantrappen and T.L. Peeters, in: Handbook of physiology, Section G., Vol. II (Am. Phys. Soc., Bethseda, MD) pp. 545–558.
5 V. Bormans, T.L. Peeters and G. Vantrappen, Regul. Peptides 15 (1986) 143.
6 T.L. Peeters, V. Bormans and G. Vantrappen, Regul. Peptides 23 (1988) 171.
7 T.L. Peeters, G. Vantrappen and I. Depoortere, in: Motilin, ed. Z. Itoh (Academic Press, San Diego, CA, 1990) pp. 93–109.
8 H. Schubert and J.C. Brown, Can. J. Biochem. 52 (1974) 7.
9 Y. Seino, J. Takeda and H. Imura, in: Motilin, ed. Z. Itoh (Academic Press, San Diego, CA, 1990) pp. 47–51.
10 P. Poitras, J.R. Reeve, M.W. Hunkapiller, L.E. Hood and J.H. Walsh, Regul. Peptides 5 (1983) 197.
11 N. Khan, A. Gräslund, A. Ehrenberg and J. Shriver, Biochemistry 29 (1990) 5743.

12 S. Edmondson, N. Khan, J. Shriver, J. Zdunek and A. Gräslund, Biochemistry 30 (1991) 11271.
13 T. Segawa, M. Nekano, Y. Kai, H. Kawatani and H. Yajima, J. Pharm. Pharmacol. 28 (1976) 650.
14 H. Yajima, Y. Kai, H. Ogawa, M. Kubota, Y. Mori and K. Koyami, Gastroenterology 72 (1977) 793.
15 T.L. Peeters, in. Bormans, I. Depoortere, G. Matthijs, K. Kitagawa and G. Vantrappen, Biomed. Res. 9 (1988) 361.
16 B. Kalman, L.B.Å. Johansson, M. Lindberg and S. Engström, J. Phys. Chem. 93 (1989) 8371.
17 P.-O. Lycksell, A. Öhman, G. Bengtsson-Olivecrona, L. Johansson, S. Wijmenga, D. Wernic and A. Gräslund, Eur. J. Biochem. 205 (1992) 227.
18 R. Rigler, C. Kristensen, J. Roslund, P. Thyberg, K. Oba and M. Eriksson, Physica Scripta T17 (1987) 204.
19 F. Claesens and R. Rigler, Eur. J. Biophys. 13 (1986) 331.
20 A.D. MacKerell Jr., R. Rigler, L. Nilsson, U. Hahn and W. Saenger, Biophys. Chem. 26 (1987) 247.
21 A. Gräslund, S.K. Kim, S. Eriksson, B. Nordén and B. Jernström, Biophys. Chem. 44 (1992) 21.
22 A.P. Demchenko, Ultraviolet spectroscopy of proteins (Springer Verlag, Berlin, 1986) pp. 124–126.
23 W.R. Laws, J. B.A. Ross, W.R. Wyssbrod, J.M. Beechem, L. Brand and J.C. Sutherland, Biochemistry 25 (1986) 599.
24 J.M. Beechem and L. Brand, Annu. Rev. Biochem. 54 (1985) 43.
25 T. Härd, K. Hsu, M.H. Sayre, E.P. Geiduschek, V. Appelt and D.R. Kearns, Biochemistry 28 (1989) 396.
26 R. Rigler, J. Roslund and S. Forsén, Eur. J. Biochem. 188 (1990) 541.
27 P. Gauduchon and P. Wahl, Biophys. Chem. 8 (1978) 87.
28 J.B.A. Ross, W.R. Laws, A. Buku, J.C. Sutherland and H.R. Wyssbrod, Biochemistry 25 (1986) 607.
29 J.R. Lakowicz, Principles of fluorescence spectroscopy (Plenum Press, New York, 1983) p. 168.